NUCL SCI TECH (2021) 32:33
https://doi.org/10.1007/s41365-021-00867-1

Study on the production characteristics of ^{131}I and ^{90}Sr isotopes in a molten salt reactor

Liang Chen[1,2,3] · Rui Yan[1,3] · Xu-Zhong Kang[1] · Gui-Feng Zhu[1] · Bo Zhou[1] · Liao-Yuan He[1] · Yang Zou[1,3] · Hong-Jie Xu[1,2,3]

Received: 12 October 2020 / Revised: 13 January 2021 / Accepted: 16 January 2021 / Published online: 22 March 2021

Abstract The production of radionuclides ^{90}Sr and ^{131}I in molten salt reactors is an attractive option to address the global shortage of radionuclides. This study evaluated the production characteristics of ^{90}Sr and ^{131}I in a modular molten salt reactor, such as equilibrium time, yield, and cooling time of isotopic impurities. The fuel burn-up of a small modular molten salt reactor was analyzed by the Triton module of the scale program, and the variation in the fission yields of the two nuclides and their precursors with burn-up time. The yield of ^{131}I and ^{131}Te has been increasing during the lifetime. ^{131}I has an equilibrium time of about 40 days, a saturation activity of about 40,300 TBq, and while ^{131}Te takes 250 min to reach equilibrium, the equilibrium activity was about 38,000 TBq. The yields of ^{90}Sr and ^{90}Kr decreased gradually, the equilibrium time of ^{90}Kr was short, and ^{90}Sr could not reach equilibrium. Based on the experimental data of molten salt reactor experiment, the amount of nuclide migration to the tail gas and the corresponding cooling time of the isotope impurities under different extraction methods were estimated. Using the HF-H_2 bubbling method, 3.49×10^5 TBq of ^{131}I can be extracted from molten salt every year, and after 13 days of cooling, the impurity content meets the medical requirements. Using the electric field method, 1296 TBq of ^{131}I can be extracted from the off-gas system (its cooling time is 11 days) and 109 TBq of ^{90}Sr. The yields per unit power for ^{131}I and ^{90}Sr is approximately 1350 TBq/MW and 530 TBq/MW, respectively, which shows that molten salt reactors have a high economic value.

Keywords Molten salt reactor · ^{90}Sr · ^{131}I · Nuclide production

1 Introduction

Radionuclides are widely used in medical treatment, metallurgy, mineral exploration, industry, and other fields. Among them, ^{90}Sr, an artificial radionuclide with a high yield in nuclear reactions, has a high application value. The nuclide can emit beta-rays with an energy of 0.546 MeV, and the penetration depth of the ray in soft tissues is 1.38 mm, which allows it to be used for skin scarring. In addition, the long-term stable power brought by ^{90}Sr's 28-year half-life makes it suitable for manufacturing nuclear batteries for long-term missions such as maritime navigation marks. Finally, the popularity of ^{90}Y radiopharmaceuticals makes it a great prospect in the production of ^{90}Sr-^{90}Y generators. According to the forecast of some institutions, the global market demand for ^{90}Sr is over $100 million per year, and ^{90}Y Ibritumomab is worth $30 million

This work was supported by the Strategic Priority Research Program of the Chinese Academy of Sciences (No. XDA02010000), Thorium Uranium Fuel Cycle Characteristics and Key Problem Research Project (No. QYZDY-SSW-JSC016), and Shanghai Natural Science Foundation (No.19ZR1468000).

✉ Rui Yan
yanrui@sinap.ac.cn

✉ Yang Zou
zouyang@sinap.ac.cn

[1] Shanghai Institute of Applied Physics, Chinese Academy of Sciences, Shanghai 201800, China

[2] School of Physical Science and Technology, ShanghaiTech University, Shanghai 201210, China

[3] University of Chinese Academy of Sciences, Beijing 100049, China

per year in sales. ^{131}I is a pure beta radionuclide with a half-life of 8.05 days. It is mainly used in the treatment of thyroid diseases and malignant tumors, as iodine can be enriched in the thyroid. Currently, there are two mature ^{131}I medical products: Na^{131}I injection and Na^{131}I capsules. With an annual sale of $400 million, ^{131}I is one of the three most sought-after radionuclides in the radiation market [1]. Simultaneously, the domestic production of medical radionuclides in China tends to be stagnant. In 2014, the import quantity of ^{131}I was as high as 20.5 kCi [2], while ^{90}Sr was mostly imported. The common production methods of radionuclides include the accelerator method, post-treatment product extraction method, reactor irradiation method [3], and reactor production method. Among them, the latter two have higher flexibility. Since 2007, the number of existing irradiation and processing facilities for medical isotopes in the world has been limited, and many of them are aging, with problems such as imminent withdrawal from the supply chain, target conversion, decommissioning and maintenance, and some planned and unplanned reactor shutdowns affect market supply [4]. Therefore, many countries have begun to develop research on the production of medical isotopes based on new reactors and processes.

Therefore, research on nuclide production based on a molten salt reactor (MSR) has also attracted people's interest after the aqueous solution reactor [5]. As one of the Generation IV reactors, the MSR has the advantages of on-line addition of fission fuel and on-line treatment of fission products because of its use of liquid fuel, which can flow in the entire main loop. Thus, the extraction of isotopes from fission products of fluorinated salts in MSRs may be an attractive technique with the feasibility of large-scale on-line mass production of isotopes. Research has indicated that for inert gases and volatile metals produced by fission, an on-line bubbling and purging device can be used to introduce a tail gas treatment system that can then be radionuclide by an electric field or spray. Chuvilin [6] and Kang [7] evaluated the potential of a MSR to produce ^{99}Mo and designed the relevant in-reactor and out-reactor extraction devices, which entered the gas phase through the gas–liquid interface and has the capacity to produce 1.96×10^6 Bq of ^{99}Mo by-products per 1 MW of electricity produced. Sheu [8] studied the production characteristics of ^{99}Mo under different core designs. Result shows that compared with HomoType and RingType, the HeteType core model, which offered superior fuel utilization and radiotoxicity minimization, was considered the most promising design. Yu [9] studied the recovery of ^{131}I from MSRs by extracting solid Te through a solid separator of a by-pass loop system (BPLS). The result shows that in a 2 MW reactor, about 155,000 Ci of ^{131}I could be produced annually. From the above, it can be concluded that many research institutions are producing radionuclides in MSRs. Additionally, there are other nuclides and methods that have potential research value.

A considerable amount of I and Sr deposits were found in the tail gas system of MSRE [10], which reveals a new method of extracting ^{90}Sr and ^{131}I from a MSR. ^{131}I exists mainly in the ionic state in the molten salt, and ^{131}Te, the precursor of ^{131}I, is a semi-soluble noble metal, half of which is dissolved in salt in the form of tellurium ions such as Te^{3-} [11] or Te^{2-} [12]. The other half enters the exhaust gas in the form of gaseous Te [10] and then decays in the trap before being collected. Furthermore, ^{131}I can be removed from the molten salt by HF-H_2 bubbling [13] and then collected by spray. ^{90}Sr and its precursor ^{90}Rb are dissolved in the salt in the form of stable fluoride, while ^{90}Kr, the precursor of ^{90}Rb, is an insoluble rare gas, which will overflow at the gas–liquid interface of the molten salt pump or be carried by helium bubbles out of the molten salt into the off-gas treatment system.

In this study, a fundamental benchmark of a small modular MSR was established. Then, critical calculation and burn-up analysis of the core physical model will be carried out by SCALE6.1. Later, the reaction chain analysis, fission yield, equilibrium concentration, yield, and cooling time of ^{90}Sr and ^{131}I nuclides, and their precursors ^{90}Kr and ^{131}Te, in the core will be launched. This provides key input data for the study of target isotope production, migration rules, and extraction methods.

2 Model and method

In this study, a thorium molten salt reactor (TMSR) with a miniaturized and modular design was studied. The entire reactor block, which contains the reactor container, core, and fuel salt, is designed as a common module which is replaced every 10 years by lifting. The thermal power of the reactor is 30 MW. One of the two molten salt loops is a fuel salt loop loaded with LiF–BeF_2–ZrF_4–UF_4–ThF_4 (compared with the chloride used in MCFR [14], the behavior of fission products in fluoride salt has been studied more maturely, hence, fluoride salt is selected here), and the other is a cooling salt loop loaded with FLiBe or FNaBe.

From inside to outside, the modular reactor core consists of the core active region, the graphite reflector, and the down-comer. A schematic diagram is shown in Fig. 1. The main parameters are listed in Table 1. The active region is composed of 127 hexagonal graphite assemblies with an edge distance of 18 cm and a height of 300 cm, of which 116 are fuel channels with an inner diameter of 6 cm, eight control rod channels, and three molten salt contact irradiation channels. The other four irradiation channels are

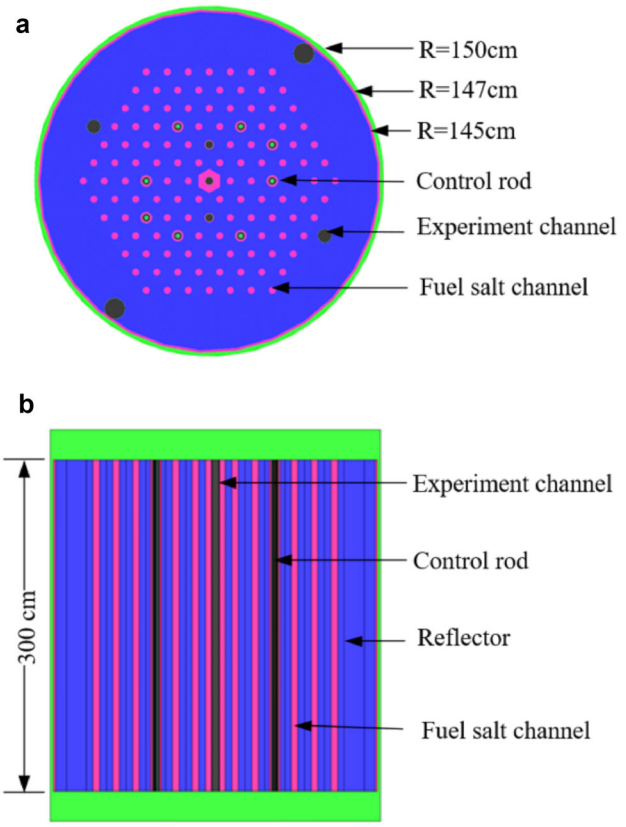

Fig. 1 (Color online) Horizontal (**a**) and vertical (**b**) sections of the core model

Table 1 Design parameters of 30 MW MSR

Parameter	Values
Thermal power (MW)	30
Fuel type	$LiF–BeF_2–ZrF_4–UF_4–ThF_4$
Uranium fuel enrichment	19.75%
Lithium-7 enrichment	99.995%
Core diameter (cm)	300
Core height (cm)	300
Reactor inlet, outlet temperature (°C)	600, 700
Upper and lower partition height (cm)	27.5

located in a reflective layer with an equivalent thickness of 35 cm formed by splicing fan-shaped assemblies. The graphite reflective layer can reduce the neutron leakage rate and slow down the fast neutrons to reduce the radiation damage to the alloy material.

SCALE [15] (Standardized Computer Analyses for Licensing Evaluation), a modular programming system, released in 1980 by Oak Ridge National Laboratory, is widely used in nuclear safety analysis and design, covering reactor criticality safety, reactor physics, radiation shielding, spent fuel and radioactive source term analysis, sensitivity and uncertainty analysis, etc. At present, it is widely used in the optimization design of water reactors and various advanced nuclear energy systems, such as gas-cooled fast reactors and MSRs [16–20]. This study is based on SCALE 6.1 updated in 2008. In the calculation, TRITON, a control module, is used for the coupling calculation of transport and fuel consumption. The functional modules involved include KENO-VI of the Monte Carlo transport program, Origen-S of the burn-up calculation module, and the corresponding coupling program.

The burn-up equation used for calculating the nuclides concentration is as follows:

$$\frac{\mathrm{d}N_i(\vec{r},t)}{\mathrm{d}t} = \beta_{i-1}N_{i-1}(\vec{r},t) - \left(\lambda_i + \sum_{g=1}^{G}\sigma_{a,g,i} + \phi_g(\vec{r},t)\right)N_i(\vec{r},t) + F_i. \tag{1}$$

Among which:

$$\beta i - 1 = \begin{cases} \lambda_{i-1} \\ \text{or} \\ \sum_{g=1}^{G}\sigma_{\gamma,g,i-1}\phi_g(\vec{r},t) \end{cases}, \tag{2}$$

$$F_i = \sum_{g'=1}^{G}\sum_{i'}\gamma_{i,i'}\sigma_{f,g',i'}\phi_{g'}(\vec{r},t), N_{i'}(\vec{r},t), \tag{3}$$

where λ is the decay constant, $\gamma_{i,i'}$ is the yield of nuclide i when nuclear fission reaction occurs on fissile nuclide i'. The first term on the right of Eq. (1) represents the rate of production of the isotope i-1 due to neutron absorption or decay, the second term represents the total loss rate of isotope i due to neutron absorption or decay, and the third term represents the rate of production due to fission reactions.

Figure 2a shows the main decay-transmutation chain of ^{131}I (the path that accounts for less than 5% of the fission yield is omitted in the figure). The fission reaction induced by thermal neutrons produces radionuclide ^{131}Sb. The vast majority decay products of ^{131}Sb are ^{131}Te, and only 6.2% of ^{131}Sb produces ^{131m}Te in the excited state when it decays, which accounts for half of all ^{131m}Te sources. The excited state of ^{131m}Te has two decay pathways. Approximately 3/4 of the ^{131m}Te is converted into ^{131}I through β-decay, and the remaining ^{131m}Te returns to the ground state ^{131}Te ($T_{1/2}$ = 25 min) by emitting internal conversion electrons. Finally, the ^{131}I produced by the two pathways generates stable ^{131}Xe through β-decay ($T_{1/2}$ = 8 d). Figure 2b shows the main decay-transmutation chain of ^{90}Sr (the path that accounts for less than 5% of the fission yield is omitted in the figure). The analysis of the decay-

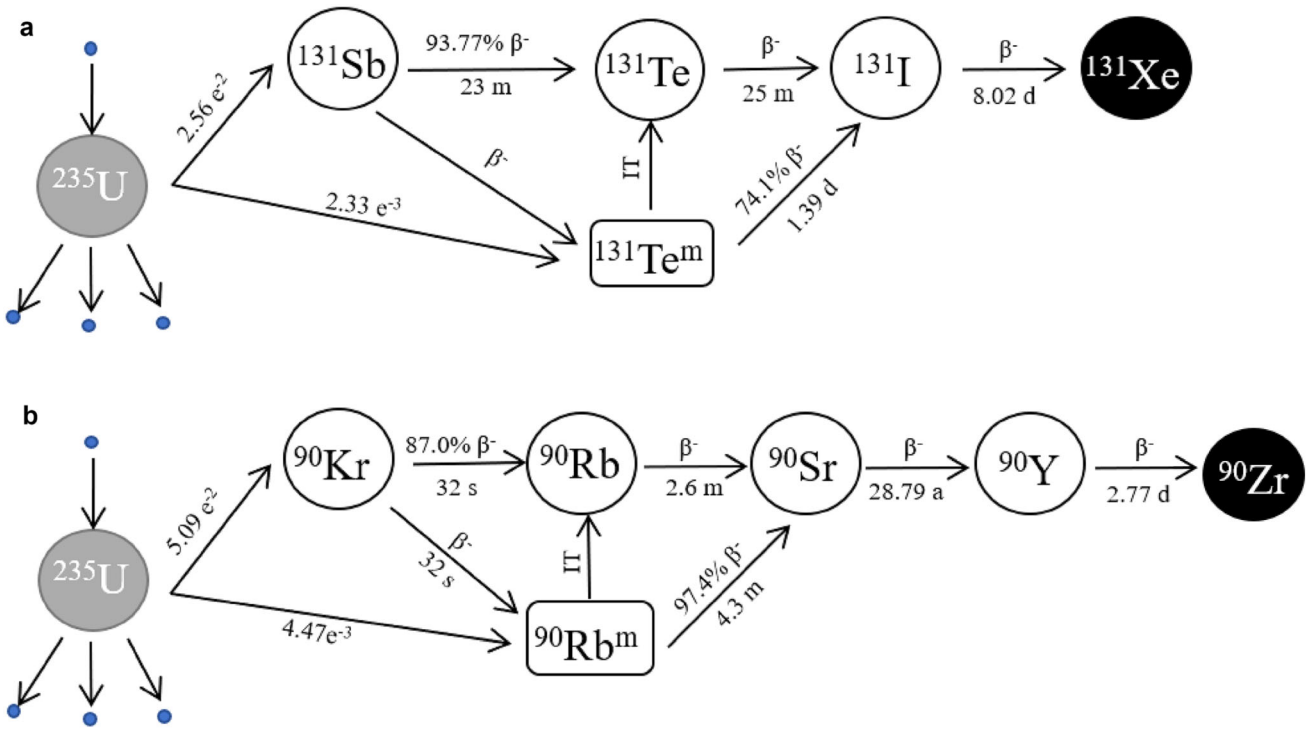

Fig. 2 Decay-transmutation chain of ^{131}I (**a**) and ^{90}Sr (**b**)

transmutation chain starts at ^{90}Kr due to the short half-life of ^{90}Br ($T_{1/2}$ = 1.92 s). When a thermal neutron bombards a ^{235}U atom to initiate a fission reaction, ^{90}Kr and a small amount of ^{90m}Rb are produced, of which 87% of ^{90}Kr produces ^{90}Rb via β-decay, and the remaining ^{90}Kr produces ^{90m}Rb. A small number (< 5%) of ^{90m}Rb produce ^{90}Rb by emitting an internal conversion electron, and most of ^{90m}Rb produces ^{90}Sr by β-decay. ^{90}Sr has a long half-life of 28.79 a, the decay product is ^{90}Y, which can be used in radiopharmaceuticals, and the final product of the decay chain is a stable nuclide-^{90}Zr.

3 Results and discussion

3.1 Yield analysis of ^{90}Sr,^{131}I, and their precursors

The reactor block was designed to be replaced once every 10 years. The fuel is not processed on-line during the entire life, but rather processed in batches after being removed as a whole. To maintain the backup reactivity required for long-life full-power operation, a higher initial fuel load is used. The initial concentration of UF_4 was 7.77%, ThF_4 was 1.78%, and the corresponding initial k_{eff} was 1.2972. As burn-up proceeds, ^{235}U is consumed, and ^{238}U and ^{232}Th absorb neutrons to produce fissionable nuclides ^{239}Pu and ^{233}U. Since there are three fissionable nuclides, and the yield of different fissionable nuclides to the target nuclides may not be the same, the variation in the total amount and percentage of fissionable nuclides in the reactor is discussed to measure the change in the average fission yield, as shown in Fig. 3. As the burn-up time increases, the fissile nuclides in the reactor are gradually consumed and the total mass continues to decrease. U is dominant in the initial charge, and the other two fissionable nuclides need to absorb neutrons before they can be produced; therefore, the proportion of ^{235}U in the entire lifetime is extremely high. However, even at the end of its life, ^{235}U accounts for more than 90% of the fissionable nuclides, whereas ^{239} Pu and ^{233} U account for only about 5%.

The thermal neutron yield data of isotopes ^{131}I, ^{131}Te, and ^{131m}Te are shown in Table 2 [21]. The independent yield is on the left, which is the yield before the β-decay but after the fission reaction. On the right is the sum of the cumulative yield, which is the independent yield and the yield of nuclides produced by β-decay. From ^{235} to ^{233}U to ^{239}Pu, the yield of fission nuclides to the same nuclides increases gradually. Among them, the independent yield of ^{131}I accounted for 0% of ^{235}U, 0.7% of ^{233}U, and 0.8% of ^{239}Pu, indicating that ^{131}I is basically derived from the decay of the precursor rather than the direct fission of the fissile nuclide, such as ^{235}U. Furthermore, the fission yields of ^{131}Te accounted for 89.3% of ^{235}U, 79.0% of ^{233}U, and 82.6% of ^{239}Pu of the cumulative yield of ^{131}I; therefore,

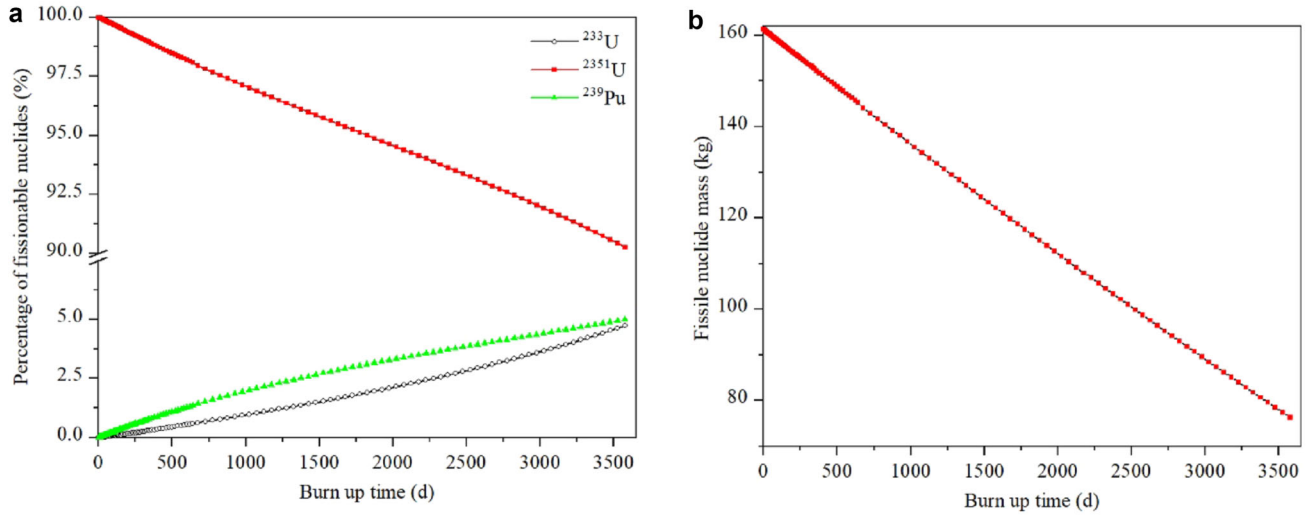

Fig. 3 Percentage (**a**) and total (**b**) change of fissile nuclides

Table 2 Fission yield of ^{131}I and its precursors

Nuclide	^{131}Te		^{131m}Te		^{131}I	
	Independent yield	Cumulative yield	Independent yield	Cumulative yield	Independent yield	Cumulative yield
^{235}U	6.79×10^{-4}	1.84×10^{-2}	1.47×10^{-3}	3.02×10^{-3}	0	2.06×10^{-2}
^{233}U	8.44×10^{-4}	1.92×10^{-2}	4.95×10^{-3}	6.28×10^{-3}	1.70×10^{-4}	2.43×10^{-2}
^{239}Pu	2.70×10^{-3}	3.17×10^{-2}	5.75×10^{-3}	8.13×10^{-3}	3.20×10^{-4}	3.84×10^{-2}

^{131}Te of the two precursors contributed most of the fission yields of ^{131}I.

Since the yields of the three fissionable nuclides to the target nuclides are different, the average cumulative yields of ^{131}I and ^{131}Te over the burn-up time of the three fissionable nuclides are studied in combination with the fission yield of the fissionable nuclides to ^{131}I and ^{131}Te, as shown in Fig. 4. The yields of ^{131}I and ^{131}Te increased continuously during the lifetime, which resulted from the increase in the contents of ^{239}Pu and ^{233}U in the fissile nuclides. The cumulative yield of ^{131}Te was approximately 3 and 10 times that of ^{235}U, respectively. Even though the yields of ^{131}I and ^{131}Te were 1.84% and 2.06%, respectively, the yields of ^{131}I and ^{131}Te reached 1.72×10^{-4} TBq/MW/s and 0.282 TBq/MW/s, respectively.

In addition, ^{131}Te has a short half-life of 25 min; therefore, it takes less time to reach equilibrium. From Fig. 5a, at around 250 min, the production rate and decay rate of ^{131}Te become balanced, and the saturation activity of ^{131}Te in molten salt is about 37,405 TBq, while the corresponding activity of ^{131m}Te is about 261 TBq. Consequently, if 50% of Te enters the gas phase, the annual ^{131}I produced by Te decay in the tail gas can reach 66,310 TBq.

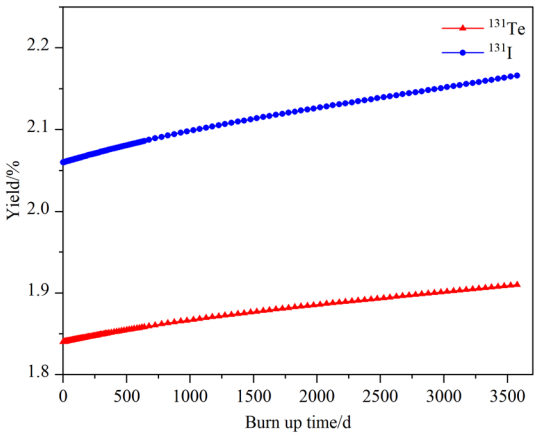

Fig. 4 Fission yield of ^{131}I and ^{131}Te varied with burn-up time

The activity changes of ^{131}I and its precursors are illustrated in Fig. 6, which shows that ^{131m}Te has the lowest activity, of only about 1/10 of that for ^{131}Te. In fact, although the yield of ^{131m}Te is less than ^{131}Te (about 20% of ^{131}Te of the total lifetime), the cumulative concentration of ^{131m}Te in the reactor is higher than ^{131}Te due to the long half-life of ^{131m}Te (about 80 times that of ^{131}Te). After reaching equilibrium, the concentration of ^{131m}Te can

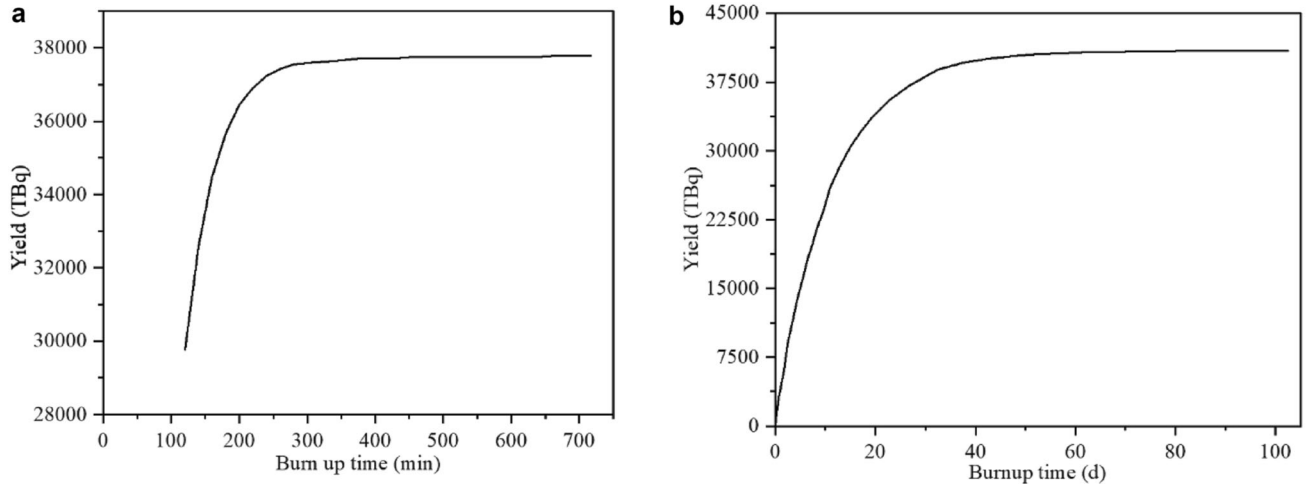

Fig. 5 Activity of ^{131}Te (**a**) and ^{131}I (**b**) varied with burn-up time

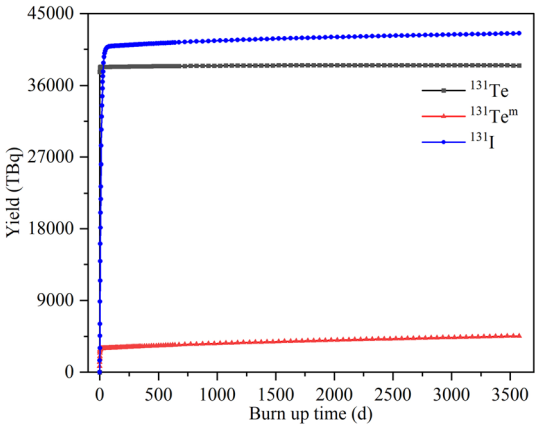

Fig. 6 Yields of ^{131}I and its precursors varied with burn-up time

reach about six times that of ^{131}Te. The activity of ^{131}I is the highest because ^{131}I is the decay product of ^{131}Te and ^{131m}Te, and ^{131}I has a longer half-life.

From Fig. 5b, the production and disappearance of ^{131}I reached equilibrium after running for about 40 days, and the equilibrium value was about 40,300 TBq. Since then, although the yield of nuclides continued to increase, as shown in Fig. 3, the yield did not change much for the total mass of fissile nuclides is decreasing. Even at the end of its life, the activity is only 1.06 times the equilibrium activity. If the HF-H_2 bubbling method is used to extract ^{131}I from molten salt, and the recovery rate is 95% [22], the annual ^{131}I that can be recovered from molten salt is 3.49×10^5 TBq.

Table 3 shows the thermal neutron fission yield of ^{90}Sr and its precursor [21]. The proportions of the independent ^{90}Sr yield of the three fissile nuclides in the cumulative yield were 2.1% (^{235}U), 6.8% (^{233}U), and 5.1% (^{239}Pu). It can be seen that ^{90}Sr mainly originates from the decay of the precursors ^{90}Rb and ^{90m}Rb. Figure 7 displays the average cumulative yield of ^{90}Kr and ^{90}Sr and the ratio of the average cumulative yield of ^{90}Kr to ^{90}Sr versus time. Figure 7b shows that the average cumulative yield of ^{90}Kr in the entire lifetime accounts for more than 80% of the average cumulative yield of ^{90}Sr, which indicates that ^{90}Kr contributes most of the ^{90}Sr yield. Therefore, most of the ^{90}Sr in the reactor was produced by the path that ^{90}Kr decays to ^{90}Rb and ^{90m}Rb, and ultimately, these two nuclides decay into ^{90}Sr. This also suggests that blowing ^{90}Kr out of the core can greatly reduce the ^{90}Sr content of the salt. The upper curve in Fig. 7a is the curve of the ^{90}Kr fission yield over the burn-up time. As the burn-up increased, the yield gradually decreased. This is mainly due to the decrease in the proportion of ^{235}U in fissile nuclides, whose contribution to yield is higher than that of the other two nuclides. Even at the end of its life, its yield is about 5.76%, which corresponds to a yield of approximately 53.7 TBq/MW/s.

Figure 8 shows the yield variation of ^{90}Sr and ^{90}Kr. The ^{90}Kr nuclide, represented by the upper curve, reaches the highest activity (about 68,000 TBq) at the first burn-up step (0.25 d), and then, the activity decreases gradually. This is mainly due to its short half-life ($T_{1/2}$ = 32 s), which is much smaller than the first burn-up step (d) chosen in the calculation. The lower curve represents the activity curve of ^{90}Sr. In contrast to the activity change of ^{90}Kr, the activity of ^{90}Sr increased slowly with the increase in running time, and the activity of ^{90}Sr did not reach equilibrium at the end of life; however, the increasing speed was obviously slowed down, and the final activity reached 10^4 TBq. This is because ^{90}Sr has a long half-life ($T_{1/2}$ = 28.79 a), which is about three times the lifetime of the reactor; hence, the disappearance rate caused by its decay is relatively small. At the same time, ^{90}Rb and ^{90m}Rb were produced and decayed in the reactor, which led to an

Table 3 Fission yield of ^{90}Sr and its precursor

Nuclide	^{90}Kr		^{90}Sr	
	Independent yield	Cumulative yield	Independent yield	Cumulative yield
^{235}U	4.66×10^{-2}	5.09×10^{-2}	1.23×10^{-3}	5.90×10^{-2}
^{233}U	4.47×10^{-2}	4.64×10^{-2}	4.46×10^{-3}	6.61×10^{-2}
^{239}Pu	1.64×10^{-2}	1.76×10^{-2}	1.23×10^{-3}	2.40×10^{-2}

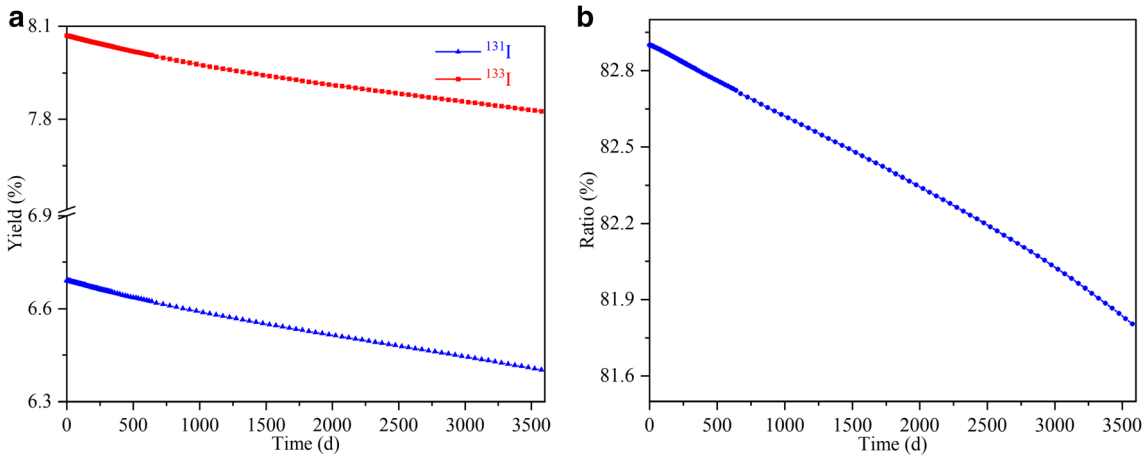

Fig. 7 Average cumulative yield of ^{90}Kr and ^{90}Sr (**a**) and the ratio of the average cumulative yield of ^{90}Kr to ^{90}Sr (**b**) versus burn-up time

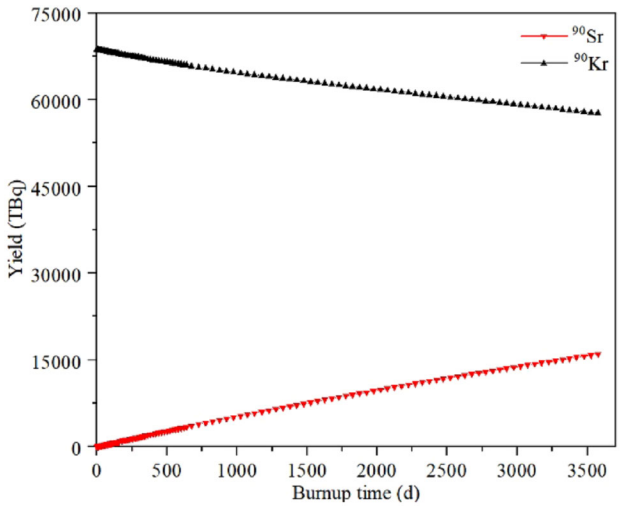

Fig. 8 Yields of ^{90}Sr and ^{90}Kr varied with burn-up time

increase in the ^{90}Sr activity. In conventional pressurized water reactors, ^{90}Sr is one of the main sources of radioactivity for reprocessing waste. Therefore, removing ^{90}Kr on-line by the bubbling method can greatly reduce the workload of post-processing [23]. If the Sr produced by Kr decay is collected directly from the exhaust gas and the time of nuclide generation to exhaust gas is ignored, the Kr overflow rate is 90% [10], and the ^{90}Sr entering the exhaust gas every year is approximately 327 TBq, which can reach 20% of ^{90}Sr activity in fuel in one year.

3.2 Effect of power on target nuclide yield

The yield of ^{131}I at different power levels is calculated because the power of the reactor may be affected by the switching of operating conditions during its lifetime. The initial concentration of ^{235}U and the mass of heavy metals corresponding to the yield in both cases are shown in Table 4. With an increase in power from 30 to 60 MW, the concentration of ^{235}U in the initial charge increases by approximately 1.03 times, corresponding to the increase in heavy metal mass, while the corresponding yield of nuclide is approximately twice the original. When the yield was normalized to the power, the results showed that the unit power yield was similar for 30 MW and 60 MW, where ^{131}I was about 1350 TBq/MW and ^{90}Sr about 530 TBq/MW.

3.3 Isotope separation

Since fission reactions produce many isotopes, and isotopes are essentially the same in nature, products collected by chemical means are bound to contain multiple isotopes. The half-life and beta-ray energy of different isotopes are generally different, for example, ^{131}I has a half-life of 8.02 days and a beta-ray energy of 970.8 keV, whereas ^{133}I has a half-life of only 20.8 h and a corresponding beta-ray energy of 1.757 MeV [21]. To accurately calculate activity and dose, medical radionuclides require high levels of isotopes. Generally, ^{131}I products require a radionuclide

Table 4 Yield of ^{131}I under different power conditions

Power (MW)	Initial U concentration	Heavy metal quality (t)	Burn-up depth GWD/MTIHM	^{131}I yield (TBq)	Unit power yield (TBq/MW)	^{90}Sr yield (TBq)	Unit power yield (TBq/MW)
30	7.77%	1.982	93.8	40,300	1343.3	15,982	532.7
60	15.85%	3.489	82.3	81,000	1350.0	31,539	525.5

impurity activity ratio of less than 0.1% [24], and the radionuclide impurity of ^{131}I is defined as the ratio of the radioactivity of ^{133}I or ^{135}I to the total radioactivity of the iodine isotope. Since ^{90}Sr originates mainly from fully cooled post-treatment waste, and ^{90}Sr has few other isotopes, there is little requirement regarding the impurity activity ratio in this report. The major isotopes with long half-lives are ^{89}Sr ($T_{1/2}$ = 50.5 d) and ^{91}Sr ($T_{1/2}$ = 9.6 h). The half-life can be cooled for a long time until the activity of the remaining isotopes is reduced to a negligible degree. The half-life of ^{131}I is only 8 day; consequently, the economic benefit will be affected if the cooling time is too long, and therefore, the minimum cooling time is discussed.

When an electric field is used to collect ^{131}Te, the Te isotopes (^{131}Te, ^{129}Te, ^{133}Te, ^{132}Te, ^{134}Te, ^{135}Te, etc.) enter the electric field in the form of gaseous Te and then decay to produce charged ions. The iodine isotope was extracted once for 250 min and then decayed for 250 min in the container (^{131}Te 10 times half-life is selected to obtain as much ^{131}I as possible). ^{129}I has a long half-life (1.57×10^7 a), and a low activity can be neglected; therefore, the remaining nuclides are all affected by a certain amount and need to be considered for cooling. Calculations show that about 0.578 TBq of ^{131}I ($T_{1/2}$ = 8.02 d) is collected in the container. Additionally, ^{132}I ($T_{1/2}$ = 2.30 h, activity before cooling = 1.07 TBq), ^{133}I ($T_{1/2}$ = 20.8 h, activity before cooling = 4.81 TBq), ^{134}I ($T_{1/2}$ = 52.5 min, activity before cooling = 15.4 TBq), and ^{135}I ($T_{1/2}$ = 6.57 h, activity before cooling = 11.5 TBq) were collected. According to the calculations, after 13 days of cooling, the ^{131}I activity will be 0.188 TBq, which is 32.5% of the initial value. The activity of ^{133}I was only 1.47×10^{-4} TBq, the activity of the remaining nuclides was approximately zero, and the ^{133}I impurity was less than 0.1%, which meets the requirements for medicinal purposes.

When the HF-H_2 bubbling method was used to extract ^{131}I from molten salt, the initial product contained ^{131}I with an activity of 4×10^4 TBq, ^{132}I with an activity of 6.25×10^4 TBq, ^{133}I with an activity of 9.37×10^4 TBq, ^{134}I with an activity of 1.11×10^5 TBq, and ^{135}I with an activity of 8.88×10^4 TBq. After 11 days of cooling of the extracted I, the activity of ^{131}I was 1.55×10^4 TBq, which was approximately 38.8% of the initial value, the activity of ^{133}I was only 14.2 TBq, and the activity of the remaining nuclides was almost zero. Therefore, the impurity of ^{133}I is less than 0.1%, which can also meet the requirements of medicine.

4 Conclusion

The radionuclides ^{131}I and ^{90}Sr are both widely used in industry and medicine. Traditional production methods, such as target irradiation or radioactive waste extraction, are costly and waste-intensive and face the problems of reactor-type aging and unscheduled shutdown with uncertain yields. If the production of these two nuclides is considered in a MSR, ^{131}I can be blown out of the molten salt in the form of HI or Te (g), and ^{90}Sr can be blown out of salt in the form of Kr.

In this study, the burn-up chains of ^{131}I and ^{90}Sr nuclides that are suitable for extraction from the reactor are arranged. ^{131}I mainly originates from the decay of ^{131}Te and ^{131m}Te, and ^{90}Sr mainly originates from the decay of ^{90}Kr, ^{90}Rb, and ^{90m}Rb. Subsequently, we analyzed the yield and the proportion of fissionable nuclides in the lifetime of a 30 MW MSR. The results show that the total amount of fissionable nuclides continues to decrease, and the proportion of ^{235}U becomes smaller, while the proportions of ^{233}U and ^{239}Pu gradually increased; however, the minimum proportion of ^{235}U was greater than 90%. Consequently, the yield changes of the target nuclides and their precursors were analyzed by combining the yield contribution and the ratio change of fissile nuclides. The results showed that the yields of ^{131}I and ^{131}Te increased gradually, while the yields of ^{90}Sr and ^{90}Kr decreased gradually.

Furthermore, we discussed the time and saturation activity required for the nuclide in the reactor to reach equilibrium activity. The equilibrium time of ^{131}I is about 40 days, and the saturation activity in salt is approximately 40,300 TBq. The equilibrium time of ^{131}Te with a slightly shorter half-life is approximately 250 min, and the equilibrium activity is 37405 TBq. Subsequently, the number of nuclides that migrate into the exhaust gas is estimated based on the migration probability in the literature. If ^{131}I is extracted from the molten salt by the HF-H_2 bubbling method, it can be recovered from the molten salt to 3.49×10^5 TBq per year and transported into tail gas to 66,310 TBq. Additionally, ^{90}Sr can be transported into tail

gas to 327 TBq per year by the helium bubbling method, which can reach 20% of ^{90}Sr activity in fuel within one year. The results show that the yield of nuclides is doubled when the power is doubled. The yield of ^{131}I and ^{90}Sr nuclides per unit power is approximately 1350 TBq and 530 TBq, respectively. Finally, the minimum cooling time of the isotope corresponding to the medicinal use is discussed, and the results showed that the impurity of I extracted by the electric field was less than 0.1% after cooling for 13 days, which could meet the medicinal requirements. The remaining ^{131}I is now 32.5% of the original. After 11 days of cooling of the extracted I collected by HF-H_2 bubbling, the remaining ^{131}I was 38.8% of the initial, and the impurities were less than 0.1%, which meets the requirements for medicinal purposes.

Author contributions All authors contributed to the study conception and design. Material preparation, data collection and analysis were performed by Liang Chen, Rui Yan, Xu-Zhong Kang, Gui-Feng Zhu, Bo Zhou, Liao-Yuan He, Yang Zou, Hong-Jie Xu. The first draft of the manuscript was written by Liang Chen, and all authors commented on previous versions of the manuscript. All authors read and approved the final manuscript.

References

1. M.Q. Li, Q.M. Deng, Z.Y. Cheng et al., Production and application of medical radionuclide: status and urgent problems to be resolved in China. J. Isotop. **26**(03), 186–192 (2013). https://doi.org/10.7538/tws.2013.26.03.0186 (**in Chinese**)
2. X.Q. Li, Z. Tang, B. Zou et al., Analysis on the imports and exports of radioisotope in China, 2010–2014. Chin. Occup Med. **43**(6), 734–742 (2016). https://doi.org/10.11763/j.issn.2095-2619.2016.06.023 (**in Chinese**)
3. M. Khalid, A. Mushtaq, Reuse of decayed tellurium dioxide target for production of iodine-131. J. Radioanal. Nucl. Chem. **299**(1), 691–694 (2014). https://doi.org/10.1007/s10967-013-2824-0
4. W. Zou, H.Y. Yin, Q. Liu, Survey on the supply of the fission 99Mo. Chin. J. Nucl. Med. Mol. Imaging. **36**(004), 375–377 (2016). https://doi.org/10.3760/cma.j.issn.2095-2848.2016.04.024 (**in Chinese**)
5. Z. Gholamzadeh, S.A.H. Feghhi, S.M. Mirvakili et al., Computational investigation of 99Mo, 89Sr, and 131I production rates in a subcritical $UO_2(NO_3)_2$ aqueous solution reactor driven by a 30-MeV proton accelerator. Nucl. Eng. Technol. **47**(7), 875–883 (2015). https://doi.org/10.1016/j.net.2015.08.004
6. D. Chuvilin, V. Zagryadskii, New method of producing 99Mo in molten-salt fluoride fuel. At. Energ. **107**(3), 185–193 (2009). https://doi.org/10.1007/s10512-010-9214-2
7. X.Z. Kang, G.F. Zhu, R. Yan et al., Evaluation of 99Mo production in a small modular thorium based molten salt reactor. Prog. Nucl. Energy. (2020). https://doi.org/10.1016/j.pnucene.2020.103337
8. R.J. Sheu, C.C. Chao, O. Feynberg et al., A fuel depletion analysis of the MSRE and three conceptual small molten-salt reactors for Mo-99 production. Ann. Nucl. Energy. **71**, 111–117 (2014). https://doi.org/10.1016/j.anucene.2014.03.031
9. C.G. Yu, X.H. Wang, C. Wu et al., Supply of I-131 in a 2 MW molten salt reactor with different production methods. Appl. Radiat. Isot. (2020). https://doi.org/10.1016/j.apradiso.2020.109350
10. E. L. Compere, E. G. Bohlmarin, S. S. Kirslis et al., Fission product behavior in the Molten Salt Reactor Experiment. ORNL, Oak ridge, 1975. https://doi.org/10.2172/4077644
11. K. Uozumi, K. Sugihara, K. Kinoshita et al., Absorption characteristics of anions (I^-, Br^-, and Te^{2-}) into zeolite in molten LiCl–KCl eutectic salt. J. Nucl. Mater. **447**(1–3), 233–241 (2014). https://doi.org/10.1016/j.jnucmat.2014.01.014
12. C.E. Bamberger, J.P. Young, R.G. Ross, The chemistry of tellurium in molten Li_2BeF_4. J. lnorg. Nucl. Chem. **36**(5), 1158–1160 (1974). https://doi.org/10.1016/0022-1902(74)80232-0
13. R.B.Bridge, MSR Program Semi-annu. Progr. Rep. Aug. 31, 1965 (ORNL, Oak ridge, 1965)
14. L.Y. He, G.C. Li, S.P. Xia et al., Effect of ^{37}Cl enrichment on neutrons in a molten chloride salt fast reactor. Nucl. Sci. Tech. **31**(3), 27 (2020). https://doi.org/10.1007/s41365-020-0740-x
15. ORNL, "SCALE: A Modular Code System for Performing Standardized Computer Analyses for Licensing Evaluations," ORNL/TM-2005/2039, Version 6.1, 2019
16. M.L. Tan, G.F. Zhu, Y. Zou et al., Research on the effect of the heavy nuclei amount on the temperature reactivity coefficient in a small modular molten salt reactor. Nucl. Sci. Tech. **30**(9), 140 (2019). https://doi.org/10.1007/s41365-019-0666-3
17. K.F. Ma, C.G. Yu, X.Z. Cai et al., Transmutation of I-129 in a single-fluid double-zone thorium molten salt reactor. Nucl. Sci. Tech. **31**(1), 10 (2020). https://doi.org/10.1007/s41365-019-0720-1
18. S.H. Yu, Q. Sun, H. Zhao et al., Conceptual design of Mars molten salt reactor. Nuclear Techniques **43**(5), 050603 (2020). https://doi.org/10.11889/j.0253-3219.2020.hjs.43.050603 (**in Chinese**)
19. D.G. Li, X.M. Zhou, G. Liu, Analysis of U-Pu breeding in molten salt fast reactor. Nuclear Techniques **43**(8), 080003 (2020). https://doi.org/10.11889/j.0253-3219.2020.hjs.43.080003 (**in Chinese**)
20. S.J. Liu, G.F. Zhu, R. Yan et al., Placement scheme of burnable poisons in a small modular fluoride-cooled high temperature reactor. Nuclear Techniques. **43**(5), 050602 (2020) https://doi.org/10.11889/j.0253-3219.2020.hjs.43.050602 (**in Chinese**)
21. N. Soppera, M. Bossant, E. Dupont, JANIS 4: an improved version of the nea java-based nuclear data information system. Nucl. Data Sheets **120**, 294–296 (2014). https://doi.org/10.1016/j.nds.2014.07.071
22. C.F. Baes, R.P. Wichner, C.E. Bamberger et al., Removal of iodide from LiF-BeF_2 melts by HF-H_2 sparging—an application to iodine removal from molten salt breeder reactor fuel. Nucl. Sci. Eng. **56**(4), 399–410 (2017). https://doi.org/10.13182/NSE75-A26685
23. B. Zhou, X.H. Yu, Y. Zou et al., Study on dynamic characteristics of fission products in 2 MW molten salt reactor. Nucl. Sci. Tech. **31**(2), 17 (2020). https://doi.org/10.1007/s41365-020-0730-z
24. IAEA, Manual of reactor produced radioisotopes. IAEA-TEC-DOC-1340, 2003